Hyperbranched Organometallic Polymers: Synthesis and Properties of Poly(ferrocenylenesilyne)s

Qunhui Sun, Kaitian Xu, Han Peng, Ronghua Zheng, Matthias Häussler, and Ben Zhong Tang*

Department of Chemistry, Institute of Nano Science and Technology, Center for Display Research, and Open Laboratory of Chirotechnology of the Institute of Molecular Technology for Drug Discovery and Synthesis,† Hong Kong University of Science & Technology, Clear Water Bay, Kowloon, Hong Kong, China

Received September 25, 2002; Revised Manuscript Received January 23, 2003

ABSTRACT: A series of hyperbranched poly(ferrocenylenesilyne)s, $[(\eta^5\text{-}C_5H_4)_2FeSi(R)]_n$ {R = CH_3 [**1**(1)], $CH{=}CH_2$ [**1**(V)], *n*-C_8H_{17} [**1**(8)], *n*-$C_{12}H_{25}$ [**1**(12)], *n*-$C_{16}H_{33}$ [**1**(16)], *n*-$C_{18}H_{37}$ [**1**(18)]}, was prepared in good isolation yields (up to 77 wt %) by one-pot coupling reactions of dilithioferrocene with trichlorosilanes. While the polymers with small R groups [**1**(1) and **1**(V)] were partially soluble, those with long alkyl chains [**1**(*m*) with $m \geq 8$] were completely soluble and readily film forming. The polymers exhibited diagnostic solution properties of hyperbranched macromolecules; for example, **1**(18) had a high absolute molecular weight ($M_w = 5 \times 10^5$ Da) but a low intrinsic viscosity ($[\eta] = 0.02$ dL/g). Spectroscopic analyses revealed that the polymers possessed rigid skeleton structures with extended conjugations, with their absorption spectra tailed into the infrared region (>700 nm). With an increase in the alkyl chain length, the polymer changed from glassy to rubbery state. The polymers lost little of their weights when heated to ∼400 °C but ceramized when pyrolyzed at higher temperatures, with ceramization yield increasing with a decrease in the alkyl chain length. Sintering **1**(1) and **1**(V) in 700−1200 °C produced ceramics in ∼50% yields. Higher temperature pyrolyses favored the formation of ceramics with bigger inorganic nanoclusters and better magnetic performances. The ceramic prepared from the calcination of **1**(1) at 1200 °C contained large iron silicide nanocrystals and exhibited high magnetizability (up to ∼51 emu/g) but near-zero remanence and coercivity. This ceramic is thus an outstanding soft ferromagnet with a high magnetic susceptibility and practically nil hysteresis loss.

Introduction

Polyalkynes are the best-known conjugated macromolecules and have attracted much interest among scientists. A rich variety of polyalkynes has been prepared in the past decades, thanks to the enthusiastic synthetic efforts of polymer chemists.[1−3] The conjugated polymers exhibit an array of exotic properties, examples of which include photoconductivity,[4] solvato- and thermochromisms,[5] radiolysis,[6] photo- and electroluminescence,[7] optical nonlinearity,[8] liquid crystallinity,[9] helical chirality or optical activity,[10] biomimetic environmental adaptability,[11] and cell growth-stimulating capability.[12] Polysilynes, a group of inorganic congeners of the organic polyalkynes, have also been created in the hot pursuit of new polymers with *new molecular structures*.[13] Indeed, although the polysilynes resemble the polyalkynes in stoichiometry [−$(RSi)_n$− vs −$(RC)_n$−], their *molecular structures* are distinctly different: the backbone of the former comprises three-dimensionally continuous silicon−silicon single bonds, whereas that of the latter consists of linear alternating carbon−carbon double bonds. The inorganic polysilynes have a random backbone structure[14] and exhibit a number of unique properties. For example, the polymers possess extensive Si−Si σ-conjugation, whose electronic absorption well extends into visible spectral region.[13,15]

In the polysilyne backbone, each silicon atom is tetrahedrally hybridized and bound via single bonds to three other silicon atoms. The resulting silicon cages are thus tight inorganic networks knitted up by the short σ bonds. Insertion of bulky moieties such as ferrocene rings into the polysilyne structures may expand the caged networks into hyperbranched spheres divergently emanating in the three-dimensional space, thus improving the solubility (and hence the processibility) of the inorganic polymers.[16−18] The mixing between the σ orbitals of the silicon atoms and the π orbitals of the ferrocene rings may confer novel electronic properties on the polymers.[19] The introduction of another kind of inorganic atom, that is, iron, into the silicon polymers may add new functionalities to the materials; for example, the polymers may show redox activity[20] and serve as precursors to magnetic ceramics.[21,22] An outstanding example in this regard is the generation of poly(ferrocenylenesilene)s by the incorporation of ferrocene rings into linear polysilene chains at the molecular level.[23,24] The hybrid offspring has exhibited an impressive array of unique material properties not accessible by the polysilene parents.[25] Molecular hybridization of the organometallic ferrocene rings with the nonlinear inorganic silicon networks has, however, been virtually unexplored.[26,27]

In this work, we utilized a coupling reaction of difunctional ferrocene with trifunctional silane and synthesized a series of hyperbranched poly(ferrocenylenesilyne)s with different organic substituents (**1**; Chart 1). In comparison to the parent inorganic polysilyne networks, the hyperbranched organometallic poly(ferrocenylenesilyne)s showed improved solubility,

* To whom correspondence should be addressed (Department of Chemistry, Hong Kong University of Science & Technology). Phone: +852-2358-7375. Fax: +852-2358-1594. E-mail: tangbenz@ust.hk.

† An Area of Excellence (AoE) Scheme supported by the University Grants Committee of Hong Kong.

10.1021/ma021529e CCC: $25.00
Published on Web 03/13/2003

Chart 1

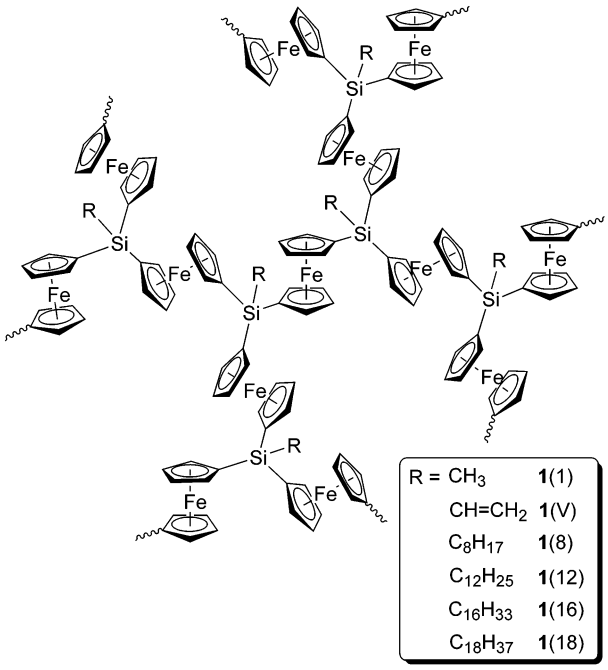

better stability, and more extended electronic conjugation. Pyrolysis of the polymers with small R substituents produced in high yields the ceramic materials consisting of metallic nanoclusters, all of which were magnetically susceptible and one of which exhibited excellent soft ferromagnetism.

Experimental Section

Materials. Ferrocene was purchased from Aldrich and was further purified by recrystallization from ethanol in our laboratory before use. The R-substituted trichlorosilanes $R-SiCl_3$ methyltrichlorosilane (Aldrich), vinyltrichlorosilane, *n*-octyltrichlorosilane, *n*-octyldecyltrichlorosilane (all from Lancaster), *n*-dodecyltrichlorosilane, and *n*-hexadecyltrichlorosilane (both from UCT) were all distilled over calcium hydride. Diethyl ether, hexane, THF (all Lab-Scan), dichloromethane (DCM; Aldrich), and *N*,*N*,*N*′,*N*′-tetramethylethylenediamine (TMEDA; Acros) were distilled from either calcium hydride or sodium benzophenone ketyl. *n*-Butyllithium (1.7 M in heptane) and all other solvents and reagents were from Aldrich and were used as received without further purification. Dilithioferrocene·TMEDA (**4**; Scheme 1) and poly[1,1′-ferrocenylene(methyl)silene] [**5**(1)] were prepared according to published experimental procedures.[24]

Instrumentation. The IR spectra of the polymers were measured on a Perkin-Elmer 16 PC FT-IR spectrophotometer. The NMR analyses were performed on a Bruker ARX 300 NMR spectrometer in deuterated chloroform using TMS as internal standard. The UV spectra were recorded on a Milton Roy Spectronic 300 array spectrophotometer, and the molar absorptivity (ϵ_{max}) was calculated on the basis of the repeat unit of the polymer. The relative molecular weights of the polymers were estimated using a size-exclusion chromatograph (SEC) system equipped with a Waters 510 HPLC pump, Ultrastyragel columns (HT3, HT4, and HT6), a column temperature controller, a Waters 486 wavelength-tunable UV−vis detector, and a Waters 410 differential refractometer (RI). THF was used as eluent at a flow rate of 1.0 mL/min. A set of monodisperse polystyrene standards covering the molecular weight range 10^2-10^7 Da was used as calibration standards. The absolute molecular weights and the intrinsic viscosities of the polymers were determined in THF by another SEC system (Waters 590) equipped with a set of parallel-series detectors, where a RI detector was connected in parallel with two series detectors: a right-angle laser light scattering (RALLS) detector and a differential viscometer (DV) detector.[28]

Scheme 1

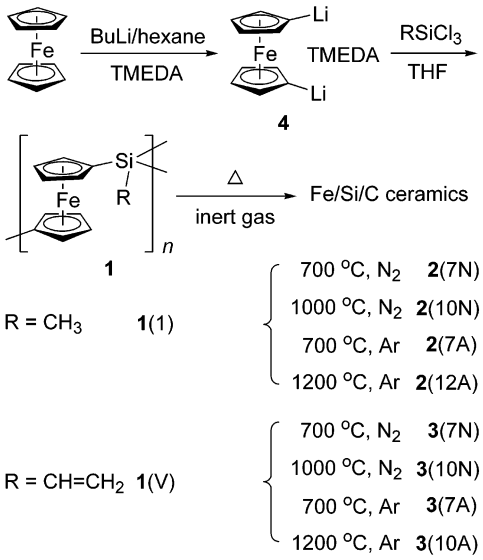

The differential scanning calorimetry (DSC) analysis was performed on a Setaram DSC 92 calorimeter at a heating rate of 10 °C/min under nitrogen. The thermogravimetric analysis (TGA) was performed at a heating rate of 20 °C/min under nitrogen using a Perkin-Elmer TGA 7 analyzer. The morphologies of the ceramization products of the polymers were imaged on a JEOL 6300 scanning electron microscope (SEM) operating at an accelerating voltage of 5 kV. The X-ray photoelectron spectroscopy (XPS) experiments were conducted on a PHI 5600 spectrometer (Physical Electronics), and the core level spectra were measured using a monochromatic Al Kα X-ray source ($h\nu = 1486.6$ eV). The analyzer was operated at 23.5 eV pass energy, and the analyzed area was 800 μm in diameter. The binding energies were referenced to the adventitious hydrocarbon C 1s line at 285.0 eV, and the curve fitting of the XPS spectra was performed using the least-squares method. The energy-dispersion X-ray (EDX) analyses were performed on a Philips XL30 SEM system with quantitative elemental mapping and line scan capacities operating at an accelerating voltage of 15 kV. The X-ray diffraction (XRD) diagrams were recorded on a Philips PW 1830 powder diffractometer using the monochromatized X-ray beam from nickel-filtered Cu Kα radiation ($\lambda = 1.5406$ Å). The magnetization measurements were carried out using a superconducting quantum interference device (SQUID) magnetometer (Quantum Design MPMS-5S) at fields ranging from 0 to 20 kOe and at temperatures of 5 and 300 K.

Polymerization. All the polymerization reactions were carried out in an atmosphere of vigorously dried nitrogen using the Schlenk technique. A typical experimental procedure for the preparation of poly[1,1′-ferrocenylene(*n*-hexadecyl)silyne] [**1**(16)] (Scheme 1) is given below as an example: Ferrocene (0.622 g), 0.6 mL of TMEDA, and 15 mL of anhydrous hexane were added into a baked 100 mL two-necked round-bottom flask at room temperature (~22 °C), into which a 2.5 M hexane solution of *n*-BuLi (2.7 mL) was carefully injected using a syringe under nitrogen with magnetic stirring. An orange slurry solution was obtained gradually. The solution was stirred for 8 h at room temperature and was then cooled to −78 °C using a dry ice/acetone bath, after which 0.8 mL of *n*-hexadecyltrichlorosilane in 50 mL of THF was added. The temperature was gradually raised from −78 °C to room temperature in 4 h. The mixture was stirred for another 20 h at room temperature, and the reaction was then terminated by adding 0.2 mL of methanol. The mixture was passed through a Pyrex filter to get rid of the fine white particles of LiCl. The filtrate was slightly concentrated and then passed through a cotton-filter into a large volume of methanol (~1000 mL) in a glass beaker under vigorous stirring. A brown thin film formed at the bottom of the beaker upon standing. After standing overnight, the methanol solvent was decanted and

Table 1. Synthesis of Hyperbranched Poly(ferrocenylenesilyne)s $-[Fc_{3/2}(R)Si]_n-$ (1)[a]

no.	R in $-[Fc_{3/2}(R)Si]_n-$	yield (wt %)	solubility[b]	M_w[c] (Da)	M_w/M_n[c]	appearance
1	CH_3 [**1**(1)]	71.1	×	2000	2.0[d]	golden yellow powder
2	$CH{=}CH_2$ [**1**(V)]	32.0	×	1300	1.6[d]	golden yellow powder
3	C_8H_{17} [**1**(8)]	67.5	√	2600	1.5	amber powder
4	$C_{12}H_{25}$ [**1**(12)]	77.0	√	6300	3.8	brown elastomer
5	$C_{16}H_{33}$ [**1**(16)]	52.0	√	9800	4.3	brown elastomer
6	$C_{18}H_{37}$ [**1**(18)]	72.3	√	11900	7.3	golden yellow powder

[a] The polymerizations of 1,1′-dilithioferrocene ($FcLi_2$) and trichlorosilanes (Cl_3SiR) were carried out under nitrogen in THF at −78 °C for 24 h. [b] Tested in common solvents (chloroform, DCM, toluene, hexane, dioxane, acetone, THF, DMF, DMSO, etc.). Symbols: × = partially soluble, √ = completely soluble. [c] Estimated by SEC in THF on the basis of a polystyrene calibration. [d] For the THF-soluble fraction.

the film became transparent. The film was put into an oven and dried under vacuum to a constant weight.

Characterization Data of the Polymers. Poly[1,1′-ferrocenylene(methyl)silyne] [1(1)]. IR KBr), ν (cm^{-1}): 3088, 2958, 2930, 2115, 1690, 1570, 1421, 1252, 1166, 1036, 776, 732. (Soluble fraction used for NMR analysis) ^1H NMR (300 MHz, $CDCl_3$), δ (TMS, ppm): 4.12 (Cp), 0.55 (Me).

Poly[1,1′-ferrocenylene(vinyl)silyne] [1(V)]. IR (KBr), ν (cm^{-1}): 3090, 2943, 1694, 1592, 1420, 1404, 1164, 1105, 1036, 958, 830, 819, 732, 693. (Soluble fraction used for NMR analysis) ^1H NMR (300 MHz, $CDCl_3$), δ (TMS, ppm): 5.5−6.2 (vinyl), 4.19 (Cp).

Poly[1,1′-ferrocenylene(*n*-octyl)silyne] [1(8)]. IR (KBr), ν (cm^{-1}): 3090, 2955, 2924, 2854, 1693, 1466, 1164, 1108, 1036, 830, 724, 684. ^1H NMR (300 MHz, $CDCl_3$), δ (TMS, ppm): 4.31 (Cp), 1.45, 1.06 (alkyl). ^{13}C NMR (75 MHz, $CDCl_3$), δ (TMS, ppm): 73.15, 70.93 (ipso-Cp), 67.73 (Cp), 34.88, 31.53, 29.31, 26.90, 25.32, 22.80, 14.22, 12.30, 11.51 (alkyl). UV (DCM): λ_{max}, 229 nm; ϵ_{max}, 8.88 × 10^3 mol^{-1} L cm^{-1}.

Poly[1,1′-ferrocenylene(*n*-dodecyl)silyne] [1(12)]. IR (KBr), ν (cm^{-1}): 3088, 2954, 2922, 2855, 1694, 1466, 1360, 1164, 1037, 1024, 829, 688. ^1H NMR (300 MHz, $CDCl_3$), δ (TMS, ppm): 4.52, 4.21 (Cp), 1.30, 0.90 (alkyl). ^{13}C NMR (75 MHz, $CDCl_3$), δ (TMS, ppm): 73.10, 70.81 (ipso-Cp), 67.91 (Cp), 31.93, 22.68, 14.09, 13.38, 2.34 (alkyl). UV (DCM): λ_{max}, 229 nm; ϵ_{max}, 8.98 × 10^3 mol^{-1} L cm^{-1}.

Poly[1,1′-ferrocenylene(*n*-hexadecyl)silynes] [1(16)]. IR (KBr), ν (cm^{-1}): 3090, 2922, 2852, 2112, 1696, 1629, 1466, 1379, 1165, 1036, 807, 722, 688. ^1H NMR (300 MHz, $CDCl_3$), δ (TMS, ppm): 4.12 (Cp), 1.26 (alkyl). UV (DCM): λ_{max}, 229 nm; ϵ_{max}, 12.49 × 10^3 mol^{-1} L cm^{-1}.

Poly[1,1′-ferrocenylene(*n*-octyldecyl)silyne] [1(18)]. IR (KBr), ν (cm^{-1}): 3091, 2923, 2853, 1692, 1672, 1467, 1379, 1165, 1037, 830, 817, 721, 688. ^1H NMR (300 MHz, $CDCl_3$), δ (TMS, ppm): 4.52, 4.22 (Cp), 1.28, 0.89 (alkyl). ^{13}C NMR (75 MHz, $CDCl_3$), δ (TMS, ppm): 73.30, 71.60 (ipso-Cp), 68.40 (Cp), 33.81, 31.88, 30.43, 30.07, 29.74, 22.63, 14.82, 13.44 (alkyl). UV (DCM): λ_{max}, 229 nm; ϵ_{max}, 15.80 × 10^3 mol^{-1} L cm^{-1}.

Ceramization. The ceramics were prepared by the high-temperature pyrolyses of the polymers under nitrogen or argon (Scheme 1). In one typical ceramization experiment conducted under nitrogen, 28 mg of poly[1,1′-ferrocenylene(methyl)silyne] [**1**(1)] was placed in a sample cell of a Perkin-Elmer TGA 7 analyzer. The sample was heated to 1000 °C at a heating rate of 10 °C/min and calcinated at the highest temperature for 1 h. A ball-shaped ceramic product [**2**(10N)] was obtained in ∼50% yield. In another typical pyrolysis experiment carried out under argon, ∼40 mg of **1**(1) was placed in a quartz tube in a Winston-Salem Thermcraft furnace, which was heated to 1200 °C at a heating rate of 10 °C/min in a stream of argon (flow rate: ∼200 cm^3/min). The sample was sintered at the highest temperature for 1 h, which gave a ceramic product [**2**(12A)] in ∼50% yield.

Characterization Data of the Ceramics. 2(7N). XPS, atomic composition (%): Fe, 10.3; Si, 21.7; C, 6.4; O, 61.6. Binding energy (eV): Fe $2p_{3/2}$, 711.7; Fe $2p_{1/2}$, 720.0, 725.1; Si 2p, 104.1. EDX, atomic composition (%): Fe, 24.0; Si, 19.8; C, 7.4; O, 48.9. XRD, 2θ (deg)/d spacing (Å): 25.25/3.52, 33.2/2.70, 35.7/2.51, 40.9/2.21, 49.5/1.84, 54.25/1.69, 62.6/1.48, 64.05/1.45, 72.05/1.31, 75.5/1.26.

2(10N). XPS, atomic composition (%): Fe, 6.1; Si, 0.7; C, 78.0; O, 15.2. Binding energy (eV): Fe $2p_{3/2}$, 707.4, 712.3; Fe $2p_{1/2}$, 720.2, 725.8; Si 2p, 104.0. EDX, atomic composition (%): Fe, 36.0; Si, 24.4; C, 30.2; O, 9.4. XRD, 2θ (deg)/d spacing (Å): 19.00/4.68, 26.90/3.31, 28.45/3.13, 32.35/2.76, 33.00/2.71, 35.65/2.52, 38.45/2.34, 43.65/2.07, 44.55/2.03, 49.50/1.84, 51.00/1.79, 51.60/1.77, 54.75/1.68, 57.50/1.60, 59.85/1.54, 66.30/1.41, 67.40/1.39.

2(7A). XPS, atomic composition (%): Fe, 12.9; Si, 19.7; C, 6.7; O, 60.7. Binding energy (eV): Fe $2p_{3/2}$, 711.2; Fe $2p_{1/2}$, 719.4, 724.9; Si 2p, 103.2. EDX, atomic composition (%): Fe, 15.5; Si, 20.3; C, 6.6; O, 57.8. XRD, 2θ (deg)/d spacing (Å): 14.15/6.25, 33.05/2.71, 35.6/2.52.

2(12A). XPS, atomic composition (%): Fe, 3.8; Si, 0.6; C, 86.7; O, 8.9. Binding energy (eV): Fe $2p_{3/2}$, 707.4, 710.8; Fe $2p_{1/2}$, 720.2, 724.8; Si 2p, 99.9, 101.5, 104.0. EDX, atomic composition (%): Fe, 43.2; Si, 29.1; C, 22.4; O, 5.3. XRD, 2θ (deg)/d spacing (Å): 26.50/3.36, 27.40/3.24, 30.40/2.94, 33.00/2.71, 35.48/2.53, 38.05/2.36, 40.75/2.21, 41.20/2.19, 45.40/2.00, 46.50/1.95, 59.95/1.54, 66.35/1.41, 69.00/1.36, 84.15/1.15.

3(7N). XPS, atomic composition (%): Fe, 14.9; Si, 15.7; C, 14.3; O, 55.2. Binding energy (eV): Fe $2p_{3/2}$, 711.4; Fe $2p_{1/2}$, 719.3, 725.1; Si 2p, 103.1. EDX, atomic composition (%): Fe, 29.1; Si, 15.8; C, 5.2; O, 50.0. XRD, 2θ (deg)/d spacing (Å): 14.5/6.10, 35.55/2.52, 40.65/2.22, 49.5/1.84, 54.1/1.69, 57.5/1.60.

3(10N). XPS, atomic composition (%): Fe, 9.1; Si, 21.0; C, 14.9; O, 55.0. Binding energy (eV): Fe $2p_{3/2}$, 711.1; Fe $2p_{1/2}$, 719.4, 724.8; Si 2p, 103.3. EDX, atomic composition (%): Fe, 27.7; Si, 18.1; C, 3.1; O, 51.2. XRD, 2θ (deg)/d spacing (Å): 24.15/3.68, 33.2/2.70, 35.7/2.51, 40.9/2.21, 49.5/1.84, 54.25/1.69, 62.6/1.48, 64.05/1.45, 72.05/1.31, 75.5/1.26.

3(7A). XPS, atomic composition (%): Fe, 17.1; Si, 16.7; C, 8.0; O, 57.8. Binding energy (eV): Fe $2p_{3/2}$, 711.4; Fe $2p_{1/2}$, 720.0, 725.0; Si 2p, 103.0. EDX, atomic composition (%): Fe, 28.1; Si, 13.0; C, 3.6; O, 55.3. XRD, 2θ (deg)/d spacing (Å): 32.70/2.74, 34.95/2.57.

3(10A). XPS, atomic composition (%): Fe, 14.7; Si, 18.4; C, 8.7; O, 58.2. Binding energy (eV): Fe $2p_{3/2}$, 711.2; Fe $2p_{1/2}$, 719.6, 724.8; Si 2p, 103.2. EDX, atomic composition (%): Fe, 30.9; Si, 16.7; C, 5.6; O, 46.9. XRD, 2θ (deg)/d spacing (Å): 14.50/6.10, 33.00/2.71, 34.95/2.57, 35.60/2.52.

Results and Discussion

Polymer Synthesis. To prepare the hyperbranched poly(ferrocenylenesilyne)s (**1**), dilithioferrocene [$(\eta^5$-$C_5H_4Li)_2Fe$ or $FcLi_2$] and trichlorosilanes (Cl_3SiR) were made to react under vigorously dried and strictly controlled polymerization conditions (Scheme 1). The coupling of $FcLi_2$·TMEDA complex with Cl_3SiCH_3 readily produced poly[1,1′-ferrocenylene(methyl)silyne] [**1**(1)] in a high yield (∼71%; Table 1, no. 1). The poly(methylsilyne) network was completely insoluble,[13] but **1**(1) was partially soluble in common organic solvents; that is, the hyperbranched polymer carrying the bulky ferrocene moieties had a better solubility. The polymerization of $FcLi_2$·TMEDA with $Cl_3SiHC{=}CH_2$ also produced a partially soluble polymer [**1**(V)], although the isolation yield of the polymer was low.

Many (partially) insoluble conjugated polymers can be made soluble by introducing long alkyl chains into their molecular structures.[29−31] Borrowing this "solvating flexible chain" concept, we incorporated long alkyl groups into the poly(ferrocenylenesilyne) structures. This strategy worked well: the polymer with flexible *n*-octyl substituents [**1**(8)] was completely soluble in common organic solvents (Table 1, no. 3). Increasing the length of the alkyl chain to 12 carbon atoms resulted in the formation of a high molecular weight polymer [**1**(12)] in a high yield (77%). Different from the polymers with short R groups, this polymer was a brown elastomer, due to a large decrease in its glass transition temperature (T_g) induced by the internal plasticizing effect of the long *n*-dodecyl group (vide infra). The elastomeric polymer easily formed shaped objects during the isolation process. When the thick films or bars of the polymer were broken, their cross sections exhibited shinny metallic luster.

We further increased the length of the alkyl chain and found that the molecular weight of the polymer monotonically increased with the alkyl chain lengthening. When the alkyl length was increased to 18, the M_w of the polymer [**1**(18)] reached a high value of ∼12 000 Da [noting that this is an SEC-estimated relative value; the absolute value was much higher (vide infra)]. Interestingly, while polymer **1**(16) was elastomeric, **1**(18) was powdery in appearance. As will be discussed later, this is probably due to the self-crystallization of the long *n*-octadecyl chains, a phenomenon often observed in the side-chain liquid crystalline polymer systems.[9,31,32]

The excellent solubility of the high molecular weight polymer **1**(18) was a particularly exciting result. It has been reported that the solubility of some polysilynes decreases with time,[13b] and we thus checked whether **1**(18) would undergo a similar solubility change. We took two approaches: one accelerated test in which a high temperature was applied and another slow test which involved a long period of time. In the accelerated test, we added ∼150 mg of the polymer to a Pyrex vacuum tube, which was sealed under vacuum and was then heated at 150 °C for 2 h. This thermal treatment resulted in little change in the solubility of the polymer. To test this quantitatively, we used a DSC apparatus to check the heat flow in situ at 150 °C isothermally. Nothing but a horizontally straight line was recorded, proving that the polymer has not undergone any chemical reactions during the heating process. For the slow test, we put a sample of **1**(18) on a shelf in our laboratory under ambient conditions. After ∼4 years, the sample was still completely soluble. The polymer thus passed both the short- and long-term tests: it remained soluble after the thermal treatment and the shelf storage.

It is well-known that SEC, when calibrated with standards of linear polymers (normally polystyrene), often underestimates the molecular weights of hyperbranched polymers.[16,17,28,33] Bianconi et al., for example, found that the molecular weights of their polysilynes estimated by SEC were ∼4 times smaller than the actual values.[13b] Recent research in the area has revealed that the underestimation can be as high as ∼30-fold for some hyperbranched polymers.[33b] We thus determined the absolute molecular weights of **1**(18) by an SEC system equipped with light scattering and viscometer detectors.[28a] The absolute M_w value given by the light scattering detector was 5×10^5 Da, much higher than the relative M_w value calibrated against the linear polystyrene standards. The intrinsic viscosity ([η]) given by the viscometer was, however, as low as 0.02 dL/g. A hyperbranched polymer with a high molecular weight often shows a low intrinsic viscosity[28,33]—polymer **1**(18) exhibited this characteristic property of a hyperbranched polymer.

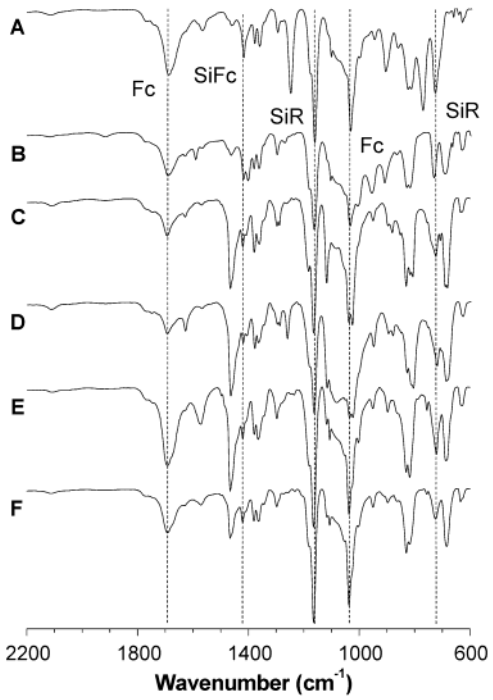

Figure 1. IR spectra of hyperbranched poly(ferrocenylenesilyne)s $-[Fc_{3/2}(R)Si]_n-$ with R = CH_3 (A), $CH{=}CH_2$ (B), *n*-C_8H_{17} (C), *n*-$C_{12}H_{25}$ (D), *n*-$C_{16}H_{33}$ (E), and *n*-$C_{18}H_{37}$ (F).

Structural Characterization. We used spectroscopic methods to analyze the molecular structures of the poly(ferrocenylenesilyne)s. Figure 1 shows their FT-IR spectra. All the polymers exhibited similar spectral profiles. Taking **1**(1) as an example, it exhibited ferrocene-associated vibration bands at 1690, 1421, and 1036 cm^{-1} and silicon bands at (1421), 1166, and 732 cm^{-1},[34] spectroscopically proving that the polymer consisted of a ferrocene ring and a silicon atom. The vinylsilyl ($CH_2{=}CH{-}Si$) moiety of **1**(V) vibrated at 1592, 1404, and 958 cm^{-1} (Figure 1B). Silane (Si−H) and siloxane (Si−O−Si) bonds are known to show very intense and broad absorption bands at ∼2200 and ∼1100 cm^{-1}.[13,34] No such bands were, however, observed at those wavenumbers in the spectra of the hyperbranched polymers.

Two broad resonance peaks at δ 4.12 and 0.55 were observed in the ^1H NMR spectrum of polymer **1**(1) (Figure 2), which can be readily assigned to the proton absorptions of the cyclopentadienyl (Cp) and methyl (Me) groups, respectively.[24,35] The repeat unit of **1**(1) comprises 1.5 ferrocenylene {$[(\eta^5\text{-}C_5H_4)_2Fe]_{3/2}$ or $(Cp_2Fe)_{3/2}$} and 1 methyl (CH_3) groups or 12 Cp and 3 Me protons. The ratio of the integrated areas of the resonance peaks of the Cp and Me protons was 1:0.26, identical (within experimental error) to the theoretical value of 12:3 (or 1:0.25). For comparison, we prepared a linear polysilene of similar structure, poly[1,1′-ferrocenylene(dimethyl)silene] [**5**(1)], according to a published procedure.[24] The linear polymer showed two resonance peaks in the Cp and Me spectral regions with a Cp/Me ratio of 1:0.76 (the theoretical ratio being 4:3

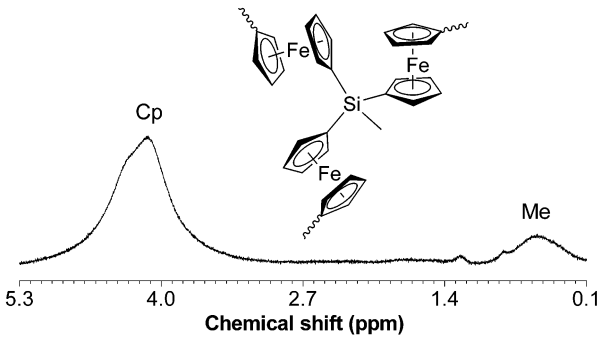

Figure 2. ^{1}H NMR spectrum of hyperbranched poly[1,1′-ferrocenylene(methyl)silyne] [**1**(1)] (soluble fraction) in chloroform-*d*.

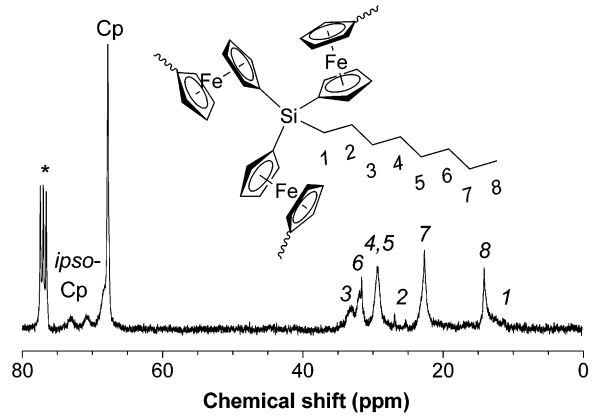

Figure 3. ^{13}C NMR spectrum of a chloroform-*d* solution of hyperbranched poly[1,1′-ferrocenylene(*n*-octyl)silyne] [**1**(8)]. The solvent peaks are marked with an asterisk (*).

or 1:0.75). The spectral profile of the linear polymer was identical to that of its hyperbranched counterpart, but the peaks of the former were better resolved than those of the latter. The absorptions of the Cp protons of **5**(1), for example, were resolved into a partially overlapping bimodal envelope with two peaks clearly discernible at δ ~4.2 and ~4.1. These two peaks were almost completely merged into one broad one in the case of **1**(1). The broadness of the absorption peak is indicative of the structural complexity of the three-dimensional hyperbranched polymer arising from the variations in the chemical environments where the protons locate.

The poor solubility of the hyperbranched polymers with small R groups made it difficult to measure their ^{13}C NMR spectra. The excellent solubility of the polymers with long alkyl groups made the job easier and enabled us to obtain ^{13}C NMR spectra of good quality, an example of which is shown in Figure 3. The ipso carbon atoms of the Cp ring gave three resonance peaks: two small but clearly observable ones at δ 73.15 and 70.93, and another partially observable one underneath the big peak of the other carbon atoms of the Cp ring. These three peaks may be associated with the absorptions of the ipso carbon atoms in the dendritic, linear, and terminal units,[28] each of which experiences a different microstructural environment, although we do not know the exact assignments of the peaks at present. The carbon atoms of the alkyl group resonated in the upfield (δ ~ 35−10). Close inspection of the carbon resonance structures revealed that the carbon atoms located closer to the silicon core gave weaker, broader "peaks", in comparison to those located far apart from the core. A similar phenomenon was observed in

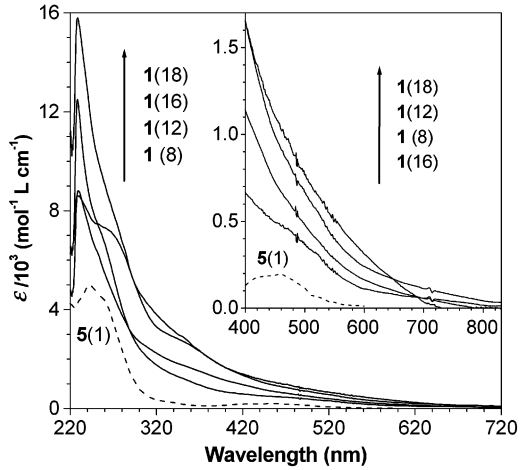

Figure 4. UV spectra of hyperbranched poly(ferrocenylenesilyne)s $-[Fc_{3/2}(n\text{-}C_mH_{2m+1})Si]_n-$ [**1**(*m*); *m* = 8−18] in DCM. The spectra of the partially soluble polymers [**1**(1) and **1**(V)] are not given because it was difficult to accurately determine their solution concentrations and molar absorptivities. The data for a THF solution of linear poly[1,1′-ferrocenylene(dimethyl)silene] [**5**(1)] are shown for comparison.

the polysilyne system, in which the resonance signal of the carbon atom directly attached to the silicon atom (C1) was completely missing or totally unobservable.[13b] This suggests that, similar to the polysilynes, our hyperbranched poly(ferrocenylenesilyne)s also possess a rigid molecular structure.

Electronic Absorption. All the soluble hyperbranched poly(ferrocenylenesilyne)s, viz., **1**(8)−**1**(18), exhibited absorption peaks in the UV spectral region, and the maximum molar absorptivity (ϵ_{max}) increased with an increase in the length of the alkyl chain (Figure 4). The absorption spectra of the polymers tailed into the infrared region (>700 nm). On the other hand, **5**(1), a linear congener of **1**, had a lower ϵ_{max} in the UV region and a shorter-wavelength band edge in the visible. The higher molar absorptivities and longer-wavelength band edges of the hyperbranched polymers indicate that they possess more extended electronic conjugations than their linear counterparts.

The absorption band edges of linear poly(diorganosilene)s {−[(RR′)Si]$_n$−; R, R′ = alkyl and/or aryl} normally do not enter the visible region irrespective of whether they are symmetrically (R = R′) or asymmetrically substituted (R ≠ R′).[13,36] The band edge of poly(di-*n*-hexylsilene) {−[(*n*-$C_6H_{13})_2$Si]$_n$−}, for example, locates in the UV region (~350 nm).[13a,b] The absorption spectra of the three-dimensional polysilyne networks were, however, tailing into the visible spectral region; for instance, the band edge of poly[(*n*-hexyl)silyne] {−[(*n*-C_6H_{13})Si]$_n$−} was at ~450 nm, which was about 100 nm red-shifted from that of its linear congener.[13a,b] This bathochromic shift was attributed to the extended Si−Si σ-conjugation across the three-dimensional polysilyne networks.[13−15] Linear poly[1,1′-ferrocenylene(methyl)silene] [**5**(1)] had a band edge in the visible (~600 nm), due possibly to the $\sigma-\pi$ conjugation[19,37] between the silene moiety and the Cp ring. The band edge of the hyperbranched poly(ferrocenylenesilyne)s further extended into the infrared with even larger extents of bathochromic shifts, probably due to the more extended $\sigma-\pi$ conjugations in the three-dimensional hyperbranched macromolecular spheres.

The poly(organosilyne)s {−[(R)Si]$_n$−; R = alkyl, aryl} were photoluminescent, emitting blue and green lights

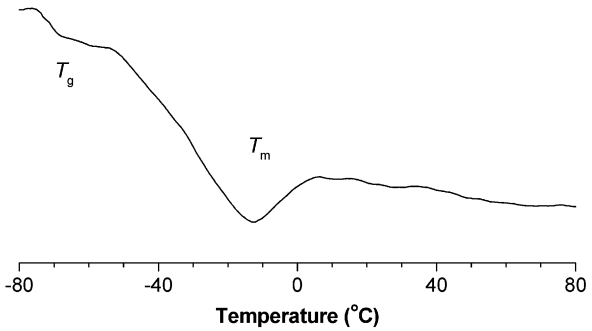

Figure 5. DSC thermogram of poly[1,1′-ferrocenylene(*n*-hexadecyl)silyne] [**1**(16)] measured under nitrogen at a heating rate of 10 °C/min during the second heating scan after the sample had been annealed at 150 °C for 10 min.

with luminescence maximums in the wavelength region of ∼440−520 nm.[15a] In sharp contrast, the hyperbranched poly(ferrocenylenesilyne)s were almost nonluminescent, though they were electronically better conjugated than their poly(organosilene) congeners. This seemed to be odd at first glance but may not be difficult to understand if we think about it twice. The better conjugation can confer high charge mobility and fast charge transport on the polymers on the positive side, but on the negative side, it may generate many defective traps that effectively quench the emission of the polymers. This is not an uncommon phenomenon in conjugated polymer systems. We have, for example, synthesized many chromophorically substituted polyacetylenes [−(RC═CR′)$_n$−] that have shorter effective conjugation lengths but are highly photo- and electroluminescent.[6,38] Their parent form, that is, the unsubstituted polyacetylene [−(HC═CH′)$_n$−], is highly conjugated but is practically nonluminescent.[39]

Thermal Transition. As shown in Table 1, the physical appearance of the poly(ferrocenylenesilyne)s changed with their R groups (from powdery to elastomeric and then back to powdery). To know the cause for this change in physical state, we investigated the thermal transitions of the polymers by DSC analyses. The polymer samples were pretreated by heating them to, and annealing at, a high temperature of 150 °C. The DSC thermograms of the polymers were recorded during the second heating scans, as a precaution against recording false signals in the heat changes associated with such events as evaporation of volatile impurities, for example, the solvents trapped inside the hyperbranched polymers. An example of the DSC curves so recorded is shown in Figure 5. The thermogram is clearly artifact-free, and from it the glass transition temperature (T_g) and the melting point (T_m) of the polymer can be readily determined.

The thermal transition parameters obtained from the DSC analyses are summarized in Table 2. The polymer with a small methyl group [**1**(1)] underwent no melting transition but a glass transition at ∼53 °C. When the R substituent changed to a "big" vinyl group, T_g decreased to 40 °C. When the number of the carbon atoms in the alkyl chains (m) increased from 8 to 18, T_g monotonically decreased from 0 to ca. −70 °C. Compared to their linear poly[1,1′-ferrocenylene(di-*n*-alkyl)silene] counterparts [**5**(m)], the hyperbranched poly[1,1′-ferrocenylene(*n*-alkyl)silyne]s [**1**(m)] exhibited higher T_g's (ΔT > 20 °C; Figure 6). This is a reflection of the rigid molecular structure of **1**: the hyperbranched polymers possess three rigid Cp rings in one of their constitutional repeat units, while the linear polymers have only two Cp rings in one of their monomer units. The T_g of **1**(m) sharply decreased with an increase in m when m was small, but the extent of change (or the slope of the T_g-m plot) became smaller when m became larger. This is probably caused by the antagonistic effect of the partial crystallization of the long alkyl chains, as will be discussed below, which hampered the segmental movements of the polymer branches.

Table 2. Thermal Properties of Hyperbranched Poly(ferrocenylenesilyne)s[a]

no.	R in −[Fc$_{3/2}$(R)Si]$_n$− (**1**)	T_g (°C)	T_m (°C)	ΔH[b] (kcal mol^{-1})	ceramic yield[c] (wt %)
1	CH_3 [**1**(1)]	53.1			62.5
2	$CH{=}CH_2$ [**1**(V)]	40.0			61.3
3	n-C_8H_{17} [**1**(8)]	0			33.1
4	n-$C_{12}H_{25}$ [**1**(12)]	−54.5	−20.5	0.91	29.9
5	n-$C_{16}H_{33}$ [**1**(16)]	−67.7	−13.8	1.15	28.5
6	n-$C_{18}H_{37}$ [**1**(18)]	−69.7	−36.7	7.76	23.6

[a] Measured under nitrogen by DSC (T_g, T_m, and ΔH) and TGA (ceramic yield) at heating rates of 10 and 20 °C/min, respectively. Fc = 1,1′-ferrocenylene. [b] Enthalpy of melting transition. [c] In the temperature region 678−687 °C.

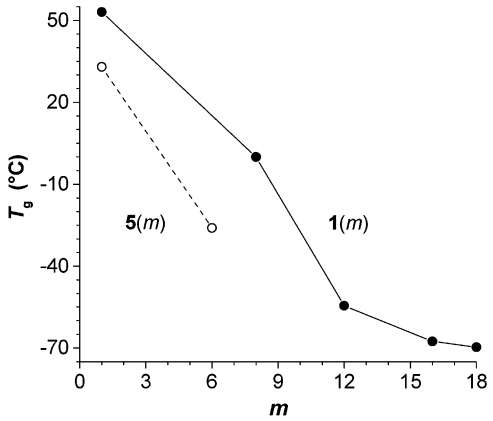

Figure 6. Change of glass transition temperature (T_g) with number of carbon atoms of alkyl chains (m) in the hyperbranched poly[1,1′-ferrocenylene(*n*-alkyl)silyne]s [**1**(m)]. Data for linear poly[1,1′-ferrocenylene(di-*n*-alkyl)silene]s [**5**(m)] are shown for comparison (data taken from refs 22 and 24).

From R = n-$C_{12}H_{25}$ (or m = 12) onward, the hyperbranched polymers [**1**(m)] started to undergo crystallization/melting transitions (Table 2, nos. 4−6). It has been observed in many liquid crystalline polymer systems that the long alkyl chain spacers and tails of their mesogenic units tend to order and eventually to crystallize, when the alkyl chain lengths become long enough.[31,40] The melting transitions observed in our hyperbranched polymers thus may be associated with the disassembling of the partially aligned or crystallized long alkyl chains. It has been noticed that the poly(alkylsilyne) with short methyl groups is apt to form irregular cagelike networks, while the polymers with long alkyl groups favor the formation of sheetlike structures,[13] which allow better steric packing. Similarly, our hyperbranched poly(ferrocenylenesilyne)s with small R groups were amorphous, while those with long alkyl chains were semicrystalline. To further verify this point, we measured the XRD patterns of the polymers.

As can be seen from Figure 7, polymer **1**(1) exhibited no sharp reflection signals but a diffuse halo peaked at a 2θ angle of ∼15°. Polymer **5**(1), an amorphous polymer and the linear congener of **1**(1), was found to show a

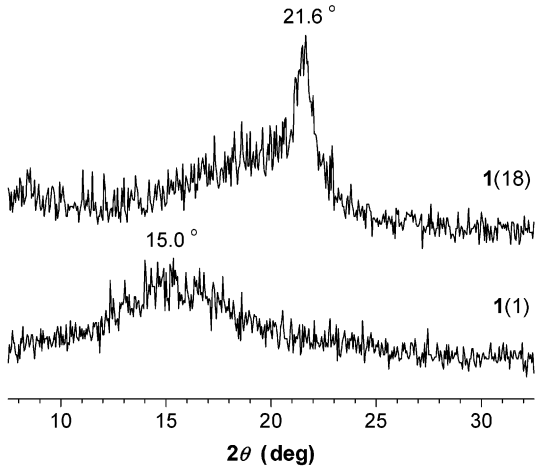

Figure 7. XRD diagrams of hyperbranched poly[1,1′-ferrocenylene(methyl)silyne] [**1**(1)] and poly[1,1′-ferrocenylene(*n*-octadecyl)silyne] [**1**(18)] measured at room temperature at a scan rate of $2\theta = 0.02°/s$.

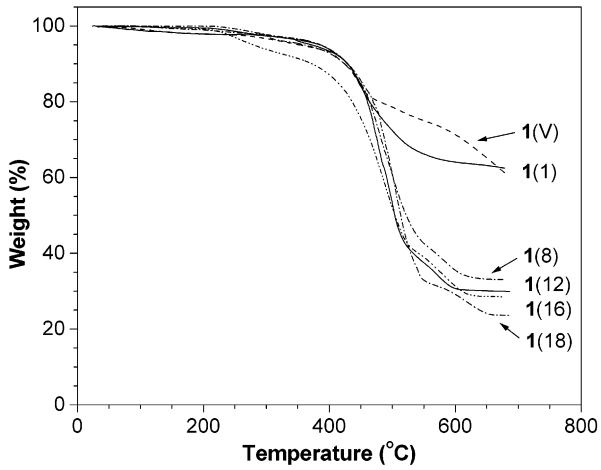

Figure 8. TGA thermograms of hyperbranched poly(ferrocenylenesilyne)s measured under nitrogen at a heating rate of 20 °C/min.

diffuse halo at a similar 2θ angle (∼14°).[41] Thus, like **5**(1), **1**(1) is also an amorphous glass at room temperature. A narrow reflection peak was, however, observed at a 2θ angle of 21.6° in the XRD diffratogram of **1**(18). The peak was not so sharp due to the imperfect packing of the alkyl chains in the crystallites. Using the Scherrer equation,[26a,42] it was calculated from the line broadening that the size of the crystallite was ∼15 nm. Obviously, the rigid skeleton structure of the hyperbranched polymer impeded the nanocrystallites from growing into big crystals of macroscopic sizes.

Pyrolytic Ceramization. The linear poly(ferrocenylenesilene)s have been utilized as organometallic polymer precursors to ceramics,[22,25,43] and we also explored the possibility of using our hyperbranched poly(ferrocenylenesilyne)s as the precursor materials.[26] We investigated the thermolysis behaviors of our polymers by TGA analyses. The polymer with methyl groups [**1**(1)] was thermally stable, losing little of its weight when heated to ∼400 °C (Figure 8). The polymer underwent a rapid thermolytic degradation in the temperature region of ∼400−500 °C, after which the TGA curve was almost leveled off. Little further weight loss was recorded when the sample was further heated to ∼680 °C, indicating that the polymer has been ceramized by the high-temperature pyrolysis. The ceramization yield of the polymer at this temperature was ∼63 wt %, much higher than that of its linear cousin **5**(1) under the comparable pyrolysis conditions (36 wt %).[22b] It is worth pointing out that **5**(1) dropped to ∼50% of its original weight when heated to 500 °C,[22b] while, at this temperature, **1**(1) still held more than 72% of its weight. This difference is obviously associated with the difference in their molecular structures. It was found that the 3D poly(organosilyne) networks were more stable than their linear poly(diorganosilene) congeners:[13a] for example, to achieve the same extent of photolysis, the network polymers require larger doses of photoirradiation.[23a] The higher ceramization yield of hyperbranched poly(ferrocenylenesilyne) **1**(1), in comparison to that of its linear counterpart **5**(1), may thus be attributed to the higher stability of the hyperbranched polymer and to the better retention of the pyrolysis-generated ceramic species inside the three-dimensional macromolecular spheres, melding of which within the cages afforded the desired ceramic product in a higher yield.

Figure 9. SEM photomicrograph of ceramic **2**(12A) prepared by pyrolysis of hyperbranched poly[1,1′-ferrocenylene(methyl)-silyne] **1**(1) at 1200 °C in an atmosphere of argon.

The pyrolysis behavior of the hyperbranched polymer with short, reactive vinyl groups [**1**(V)] was similar to that of **1**(1). Its ceramization yield at the high temperature was also high (∼61 wt %). Though the polymer with the long *n*-octyl chains [**1**(8)] commenced to lose its weight at a temperature similar to that of **1**(1) or **1**(V), its ceramization yield was much lower, being only ∼33 wt % at ∼680 °C. A further increase in the alkyl chain length led to a further decrease in the ceramization yield. From the pyrolysis of **1**(18) at ∼690 °C, a ceramic product was obtained in a yield as low as ∼24 wt %. Clearly, the long alkyl chains are detrimental to the ceramization of the hyperbranched polymers.

Since the TGA analyses showed that the polymers with small methyl [**1**(1)] and vinyl groups [**1**(V)] were promising precursor candidates for ceramics, we further studied their ceramization processes. We heated the polymers to high temperatures (700−1200 °C) and isothermally sintered the samples at the high temperatures under an inert gas atmosphere (Scheme 1), which afforded ceramic products in ∼50 wt % yields. As shown in Figure 9, the ceramic produced by the calcination of polymer **1**(1) at 1200 °C under argon [**2**(12A)] was mesoporous in morphology, comprising many three-dimensionally tortuously interconnected clusters with sizes of a few hundred nanometers. This morphological structure suggests such a process of ceramization: the pyrolytic decomposition strips off some of the organic moieties from the skeletons of the hyperbranched polymer spheres and the fast evaporation of the volatile

fragments at the high temperature leaves behind the mesoscopic pores. In the meantime, the naked reactive inorganic residues undergo heavy cross-linking reactions to aggregate into the nanoscopic clusters, forming the basic components of the ceramic product.

Ceramic Composition. We used XPS and EDS techniques to analyze the ceramic products in an effort to learn their chemical compositions. Similar to the ceramics prepared from the pyrolyses of the linear poly(ferrocenylenesilene)s,[22,25] the ceramics from our hyperbranched poly(ferrocenylenesilyne)s all contained iron, silicon, carbon, and oxygen species. The combined XPS and EDX analyses revealed that the oxygen contents of the ceramics decreased from the surfaces to the bulks, suggesting that the oxygenic species were formed by the reactions of the oxygen and moisture absorbed on the surfaces of the polymer precursors during the ceramization processes and/or by the postreactions of oxygen and moisture with the surfaces of the ceramic products during the handling and storage processes. The latter possibility is supported by the observations that many metallic nanoclusters can be readily oxidized in a split second.[44] Moving inward from the surfaces to the bulks, the iron contents of the ceramics increased, while their carbon contents decreased. For example, the atomic composition of iron of **2**(12A) increased from a low surface value of ~4% (measured by XPS) to a high bulk value of ~43% (by EDX analysis). On the contrary, its atomic composition of carbon decreased from ~87% (on the surface) to ~22% (in the bulk). This suggests that the ceramization process started from the formation of the iron nanocluster inner cores, onto which other ceramic species were depositing along with the progress of the pyrolytic cross-linking reaction.

The surface and bulk iron contents of the ceramics prepared under different conditions varied in the ranges ~4−17% (XPS) and ~15−43% (EDS), respectively, both of which are much higher than those (1% by XPS and 11% by EDX analysis) of the ceramic prepared from the pyrolysis of linear **5**(1) at a similarly high temperature (1000 °C) under inert gas atmosphere.[22] For the linear polymer, cutting a few bonds will significantly decrease its molecular weight and generate volatile ferrocenyl fragments, evaporation of which at the high-temperature results in the loss of the iron species. On the other hand, the molecular weight of our hyperbranched polymers would not change much by cleaving a few bonds due to their three-dimensional topological structures. The retention of the high molecular weight branches and the confinement of the ferrocenylene moieties in the hyperbranched spheres allow the iron species to have more time to take part in the cross-linking reactions, hence enhancing their chances to transform into the nonvolatile inorganic agglomerates.

To gain insights into the chemical structures of the iron species in the ceramic products, we inspected their Fe 2p core level photoelectron spectra. Examples of the Fe 2p photoelectron spectra of ceramics **2** and **3** are given in Figure 10. The ceramic produced by the pyrolysis of **1**(1) at 1200 °C [**2**(12A)] exhibited, in addition to the noisy tails in the high binding energy region, three major peaks at 720.2, 710.8, and 707.4 eV, which are the Fe $2p_{1/2}$ peak of the iron atom and the Fe $2p_{3/2}$ peaks of Fe_3O_4 and Fe_3Si species, respectively.[26,45] On the other hand, the ceramic obtained from the pyrolysis of polymer **1**(V) at 1000 °C, viz., **3**(10A), displayed two main peaks at 724.8 and 711.2 eV, which

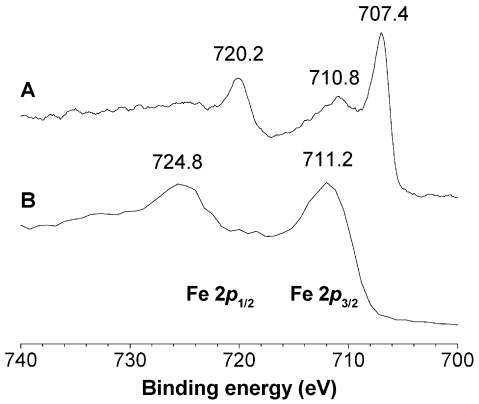

Figure 10. Fe 2p photoelectron spectra of ceramics (A) **2**(12A) and (B) **3**(10A) prepared by pyrolytic ceramizations of hyperbranched (A) poly[1,1′-ferrocenylene(methyl)silyne] [**1**(1)] at 1200 °C and (B) poly[1,1′-ferrocenylene(vinyl)silyne] [**1**(V)] at 1000 °C under argon.

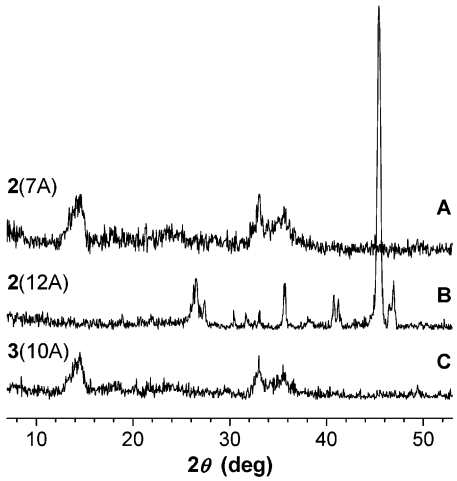

Figure 11. XRD diffractograms of ceramics (A) **2**(7A), (B) **2**(12A), and (C) **3**(10A).

are associated with the Fe $2p_{1/2}$ and Fe $2p_{3/2}$ core level binding energies of Fe_3O_4 and Fe_2O_3, respectively.[26,45] Thus the ceramics prepared from different precursor polymers under different sintering conditions can have quite different chemical compositions.

To collect more information on the bulk compositions of the ceramic materials, we measured their XRD patterns. While the precursor polymers **1**(1) and **1**(V) were amorphous (cf., Table 2 and Figure 7), their ceramic products exhibited XRD diagrams with many Bragg reflection peaks, suggesting that they contain different crystalline species. We used the data files in the databases of the Joint Committee on Powder Diffraction Standards of the International Center for Diffraction Data (JCPDS-ICDD) to identify the reflections; for instance, the peaks at 2θ angles of 14.15° and 35.60° in the diffractogram of **2**(7A) (Figure 11A) are associated with the reflections of γ-$Fe_2O_3 \cdot H_2O$ and γ-Fe_2O_3 crystals, according to the ICDD data files 02-0127 and 25-1402, respectively. The reflection peaks were, however, broad, suggesting that the crystallites are imperfect in packing and small in size. Using the full widths at half-maximums of the reflection peaks, it was calculated from the Scherrer equation that the sizes of the γ-$Fe_2O_3 \cdot H_2O$ and γ-Fe_2O_3 crystallites were ~9 and ~7 nm, respectively, similar to those of the iron oxide nanoparticles in the ceramics prepared from the

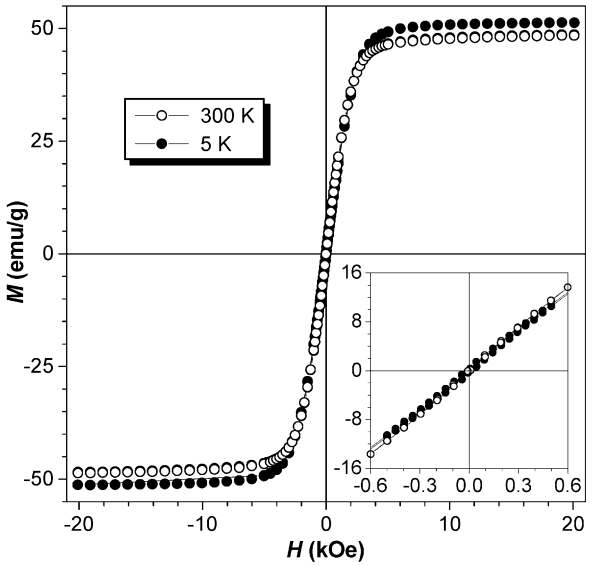

Figure 12. Plots of magnetization (M) versus applied magnetic filed (H) at 300 and 5 K for ceramic **2**(12A). Inset (lower right panel): enlarged portion of the plots in the low magnetic field region.

pyrolyses of the linear poly(ferrocenylenesilene)s (∼2−20 nm).[22,24,43]

The reflection peaks of the ceramic prepared at a higher temperature of 1200 °C, that is, **2**(12A), were much sharper, indicating that the ceramic contains bigger crystals. Among the many peaks in the XRD diagram, the most outstanding one was the intense peak of iron silicide (Fe_3Si) crystal at a 2θ angle of 45.4° (ICDD data file 45-1207). Its size calculated from the Scherrer equation was as big as ∼37 nm. This ceramic also contained γ-Fe_2O_3 crystal (2θ = 35.5°), whose reflection was, however, better defined and whose size was much bigger (∼60 nm). Thus, the calcination at the higher temperature facilitated the crystallites to grow into bigger sizes, in agreement with the early observations of Manners and Ozin's groups.[22,24,43]

The diffractogram of **3**(10A) was similar to that of **2**(7A); thus, although **3**(10A) was prepared at a higher temperature (1000 °C), it contained small nanocrystallites. The high reactivity or polymerizability of the vinyl groups may have enabled **1**(V) to undergo cross-linking reactions at lower temperatures, and this early formation of carbonaceous network structures may have obstructed the metallic species to enter the crystalline lattices in the latter ceramization stage at the high temperatures, hence hampering them from growing into bigger crystals.

Magnetic Susceptibility. It has now become clear that all the ceramic materials contain nanoscopic iron species, which are thus expected to be magnetically active. This was indeed the case: the ceramics were attracted to a bar magnet at room temperature; that is, they were readily magnetizable. We thus used the SQUID technique to investigate their magnetization behaviors in externally applied magnetic fields (with field strength up to 20 kOe) at different temperatures (300 and 5 K). The magnetization curves for ceramic **2**(12A) are shown in Figure 12 as an example, and the magnetic properties of all the ceramic materials are summarized in Table 3.

When placed in a magnetic field at a temperature close to room temperature (300 K), **2**(12A) was swiftly magnetized, as evidenced by an immediate raise in its magnetization curve (Figure 12). The magnetization rapidly increased with an increase in the strength of the applied field and became leveled off at a field strength of ∼5 kOe. When the temperature was decreased to 5 K, the magnetization was enhanced, and the saturation magnetization (M_s) went up to ∼51 emu/g, close to the value for bulk γ-Fe_2O_3 maghemite (74 emu/g).[46] To see whether there exists any hysteresis in the magnetization process of **2**(12A), we enlarged its magnetization curves in the low field region. As can be seen from the inset of Figure 12, even at the high magnification, no hysteresis loops can be identified: the magnetization plots crossed right through the zero point, when the magnetization experiments were carried out at either 300 or 5 K. Clearly, no remanence and coercivity were observable in the magnetization of **2**(12A).

Table 3. Magnetic Properties of Ceramics 2 and 3

		300 K[b]			5 K[b]		
no.	ceramic[a]	M_s	M_r	H_c	M_s	M_r	H_c
1	**2**(7N)	7.3	0.9	0.19	8.9	3.4	0.61
2	**2**(10N)	15.9	2.6	0.65	21.3	6.4	0.18
3	**2**(7A)	5.0	0.3	0.50	7.3	1.6	0.43
4	**2**(12A)	48.6	∼0	∼0	51.3	∼0	∼0
5	**3**(7N)	9.6	∼0	∼0	13.0	3.1	0.54
6	**3**(10N)	12.1	1.3	0.11	14.8	5.1	0.60
7	**3**(7A)	9.7	∼0	∼0	13.1	2.6	0.59
8	**3**(10A)	10.8	2.0	0.27	13.2	4.6	0.67

[a] Fabricated by pyrolysis at a high temperature (700, 1000, or 1200 °C) in an inert gas atmosphere (nitrogen or argon). [b] Abbreviations: M_s (emu/g) = saturation magnetization (in an external field of 20 kOe), M_r (emu/g) = magnetic remanence (at zero external field), and H_c (kOe) = coercivity (at zero magnetization).

Not all the ceramics, however, behaved like **2**(12A). The ceramics fabricated from different precursor polymers under different pyrolysis conditions performed magnetically differently. The ceramic prepared from the pyrolysis of precursor **1**(1) at 700 °C under nitrogen [**2**(7N)] exhibited a low M_s of ∼7 emu/g in a magnetic field of 20 kOe at 300 K (Table 3, no. 1). A hysteresis loop was observed in the magnetization process, although both remanence M_r (<1 emu/g) and coercivity H_c (∼0.2 kOe) were low. When the magnetization temperature was decreased to 5 K, all the magnetization parameters were increased. The ceramic prepared from **1**(1) at a higher temperature [1000 °C; **2**(10N)] performed better magnetically than its counterpart prepared at the low temperature [**2**(7N)]: the M_s values of the former were more than 2-fold higher than those of the latter at both 300 and 5 K.

A similar but more profound effect of pyrolysis temperature was observed when the ceramics prepared under argon were magnetized. Like **2**(7N), **2**(7A) was also poorly magnetic, and its M_s values were in the range of ∼5−7 emu/g. The ceramic prepared at the high temperature of 1200 °C [**2**(12A)] was, however, a much stronger magnet, whose M_s values were ∼10- and ∼7-fold higher than those of **2**(7A) at 300 and 5 K, respectively. The better magnetic performances of the ceramics prepared at the higher temperatures may be associated with their bigger crystal sizes. A small crystal possesses a large area of surface, on which the discontinuity of the superexchange bonds between the iron species leads to the formation of canted spins.[47] The noncollinear spin structures due to the pinning of the

surface spins at the interfaces of the magnetic nanoclusters and the nonmagnetic ceramic surroundings reduce the total magnetic moments of the nanoclusters, resulting in a decrease in their magnetizability.[47,48] The bigger crystals have smaller surface areas and hence higher magnetic susceptibilities.

The magnetization behaviors of the ceramics fabricated from polymer **1**(V), viz. **3**, were similar to those of **2** in one aspect but different in the other. Similarly, higher pyrolysis temperature again favored the formation of ceramics with higher magnetizabilities: the M_s values of the ceramics prepared at 1000 °C were always higher than those of the ceramics prepared at 700 °C. However, different from **2**, none of ceramics **3** exhibited a really high magnetizability. The M_s values of the ceramics prepared at the high pyrolysis temperature (1000 °C), that is, **3**(10N) and **3**(10A), were moderate at the low magnetization temperature (5 K), being in the range of ∼13−15 emu/g. These values are, however, still much higher than those of the ceramics prepared from the pyrolyses of linear polymer **5**(1), which were in the range of 0.52−3.5 emu/g.[22,24,43] This difference in magnetizability may be caused by the difference in their iron contents: the atomic compositions of iron in **3** were ∼28−31% (by EDX analysis), while those in the ceramic prepared from the linear polymer precursor were only 11% (also by EDX analysis).[22]

Ceramics **3**(7N) and **3**(7A) exhibited typical superparamagnetic behavior:[49] there were practically no hysteresis loops in their magnetization curves at 300 K, but well-defined loops were observed when the magnetization was carried out at 5 K (Table 3, nos. 5 and 7). Remarkably, however, **2**(12A) did not show any hysteresis loops even when it was magnetized at 5 K (Table 3, no. 4). In other words, this ceramic does not suffer any magnetic hysteresis loss at either high or low temperature. Silicon steel (Si−Fe) is widely used in the electromagnetic systems (generators, motors, transformers, solenoids, etc.) because of its very low magnetic hysteresis loss.[50,51] The XRD analysis has revealed that the major component of the iron nanoclusters in **2**(12A) is the iron silicide (Fe_3Si) species (cf., Figure 11B), which may be the cause for its near-zero M_r and H_c values. This ceramic material is thus an outstanding soft ferromagnet with a high magnetic susceptibility (M_s: ∼51 emu/g) and low hysteresis loss (M_r and H_c: practically nil).

Concluding Remarks

In this work, we generated a group of new hyperbranched organometallic polymers by molecularly fusing the ferrocenylene and silyne moieties into a three-dimensional macromolecular structure. The poly(ferrocenylenesilyne)s were readily synthesized by a one-pot experimental procedure in good isolation yields. The properties of the polymers changed with the alkyl substituents on the silicon atom: with an increase in the length of the alkyl chain, the solubility of the polymer increased, while its T_g and ceramization yield decreased. The pyrolysis temperature affected the structure and properties of the resultant ceramic materials: sintering polymers **1**(1) and **1**(V) at higher temperatures produced ceramic materials with bigger iron nanoclusters and higher magnetic susceptibilities. Pyrolyzing **1**(1) at 1200 °C under argon resulted in the formation of an outstanding soft ferromagnetic ceramic, that is, **2**(12A), which was magnetically highly susceptible but practically hysteresis-free in its magnetization processes.

In comparison to the poly(alkylsilyne) networks, our hyperbranched poly(ferrocenylenesilyne)s were electronically more conjugated, with their absorption band edges entering the infrared spectral region, due probably to the extended $\sigma-\pi$ conjugation in the three-dimensional macromolecular spheres. Compared to their linear poly(ferrocenylenesilene) cousin **5**(1), hyperbranched polymers **1**(1) and **1**(V) produced, upon sintering at the high temperatures, the ceramics with higher iron contents and bigger nanocrystals in higher ceramization yields, thanks to the better retention of the pyrolysis-generated ceramizing species inside the macromolecular cages. Our hyperbranched polymers are thus a group of better precursor polymers for the fabrication of nanostructured magnetoceramics.

Acknowledgment. We acknowledge the financial support of the Hong Kong Research Grants Council (Project Nos.: HKUST 6187/99P, 6121/01P, and 6085/02P) and of the University Grants Committee of Hong Kong through an Area of Excellence Scheme (Project No. AoE/P-10/01-1-A). We also appreciate the technical assistance and helpful discussions of the technical staff in the Materials Characterization & Preparation Facility of our University.

References and Notes

(1) (a) Shirakawa, H. *Angew. Chem., Int. Ed.* **2001**, *40*, 2575−2580. (b) MacDiarmid, A. G. *Angew. Chem., Int. Ed.* **2001**, *40*, 2581−2590. (c) Heeger, A. J. *Angew. Chem., Int. Ed.* **2001**, *40*, 2591−2611.

(2) (a) Masuda, T.; Higashimura, T. *Adv. Polym. Sci.* **1987**, *81*, 121. (b) Novak, B. M.; Risse, W.; Grubbs, R. H. *Adv. Polym. Sci.* **1992**, *102*, 47−72. (c) Ginsburg, E. J.; Gorman, C. B.; Grubbs, R. H. In *Modern Acetylene Chemistry*; Stang, P. J., Diederich, F., Eds.; VCH: New York, 1995; Chapter 10, pp 353−383. (d) Tabata, M.; Sone, T.; Sadahiro, Y. *Macromol. Chem. Phys.* **1999**, *200*, 265−282. (e) Reddinger, J. L.; Reynolds, J. R. *Adv. Polym. Sci.* **1999**, *145*, 57−122. (f) Choi, S. K.; Gal, Y. S.; Jin, S. H.; Kim, H. K. *Chem. Rev.* **2000**, *100*, 1645−1681. (g) Yashima, E. *Anal. Sci.* **2002**, *18*, 3−6.

(3) (a) Tang, B. Z.; Xu, K.; Sun, Q.; Lee, P. P. S.; Peng, H.; Salhi, F.; Dong, Y. *ACS Symp. Ser.* **2000**, *760*, 146−164. (b) Tang, B. Z.; Cheuk, K. K. L.; Salhi, F.; Li, B.; Lam, J. W. Y.; Cha, J. A. K.; Xiao, X. *ACS Symp. Ser.* **2001**, *812*, 133−148. (c) Cheuk, K. K. L.; Li, B.; Tang, B. Z. *Curr. Trends Polym. Sci.* **2002**, *7*, 41−55.

(4) (a) Tang, B. Z.; Chen, H.; Xu, R.; Lam, J. W. Y.; Cheuk, K. K. L.; Wong, H. N. C.; Wang, M. *Chem. Mater.* **2000**, *12*, 213−221. (b) Sun, J.; Chen, H.; Xu, R.; Wang, M.; Lam, J. W. Y.; Tang, B. Z. *Chem. Commun.* **2002**, 1222−1223.

(5) (a) Tang, B. Z.; Poon, W. H.; Peng, H.; Wong, H. N. C.; Ye, X.; Monde, T. *Chin. J. Polym. Sci.* **1999**, *17*, 81−86. (b) Tang, B. Z. *Polym. News* **2001**, *26*, 262−272. (c) Chen, J.; Xie, Z.; Lam, J. W. Y.; Law, C. C. W.; Tang, B. Z. *Macromolecules* **2003**, *36*, 1108−1117.

(6) (a) Tang, B. Z.; Masuda, T.; Higashimura, T.; Yamaoka, H. *J. Polym. Sci. Polym. Phys. Ed.* **1990**, *28*, 281−292. (b) Tang, B. Z.; Masuda, T.; Higashimura, T.; Yamaoka, H. *J. Polym. Sci. Polym. Chem. Ed.* **1989**, *27*, 1197−1209.

(7) (a) Xie, Z.; Lam, J. W. Y.; Dong, Y.; Qiu, C.; Kwok, H. S.; Tang, B. Z. *Opt. Mater.* **2002**, *21*, 231−234. (b) Lam, J. W. Y.; Law, C. K.; Dong, Y.; Wang, J.; Ge, W.; Tang, B. Z. *Opt. Mater.* **2002**, *21*, 321−324. (c) Huang, Y.; Ge, W.; Lam, J. W. Y.; Tang, B. Z. *Appl. Phys. Lett.* **2001**, *78*, 1652−1654. (d) Huang, Y. M.; Lam, J. W. Y.; Cheuk, K. K. L.; Ge, W.; Tang, B. Z. *Macromolecules* **1999**, *32*, 5976−5978. (e) Tang, B. Z.; Xu, H.; Lam, J. W. Y.; Lee, P. P. S.; Xu, K.; Sun, Q.; Cheuk, K. K. L. *Chem. Mater.* **2000**, *12*, 1446−1455.

(8) Tang, B. Z.; Xu, H. *Macromolecules* **1999**, *32*, 2569−2576.

(9) (a) Lam, J. W. Y.; Luo, J.; Dong, D.; Cheuk, K. K. L.; Tang, B. Z. *Macromolecules* **2002**, *35*, 8288−8299. (b) Lam, J. W. Y.; Dong, Y.; Cheuk, K. K. L.; Luo, J.; Xie, Z.; Kwok, H. S.; Mo, Z.; Tang, B. Z. *Macromolecules* **2002**, *35*, 1229−1240. (c)

Tang, B. Z.; Lam, J. W. Y.; Luo, J.; Dong, Y.; Cheuk, K. K. L.; Xie, Z.; Kwok, H. S. *Proc. SPIE* **2001**, *4463*, 132−138. (d) Lam, J. W. Y.; Kong, X.; Dong, Y.; Cheuk, K. K. L.; Xu, K.; Tang, B. Z. *Macromolecules* **2000**, *33*, 5027−5040.

(10) (a) Tang, B. Z.; Kotera, N. *Macromolecules* **1989**, *22*, 4388−4390. (b) Xu, K.; Peng, H.; Lam, J. W. Y.; Poon, T. W. H.; Dong, Y.; Xu, H.; Sun, Q.; Cheuk, K. K. L.; Salhi, F.; Lee, P. P. S.; Tang, B. Z. *Macromolecules* **2000**, *33*, 6918−6924. (c) Salhi, F.; Cheuk, K. K. L.; Sun, Q.; Lam, J. W. Y.; Cha, J. A. K.; Li, G.; Li, B.; Luo, J.; Chen, J.; Tang, B. Z. *J. Nanosci. Nanotechnol.* **2001**, *1*, 137−141.

(11) (a) Li, B.; Cheuk, K. K. L.; Ling, L.; Chen, J.; Xiao, X.; Bai, C.; Tang, B. Z. *Macromolecules* **2003**, *36*, 77−85. (b) Li, B.; Cheuk, K. K. L.; Salhi, F.; Lam, J. W. Y.; Cha, J. A. K.; Xiao, X.; Bai, C.; Tang, B. Z. *Nano Lett.* **2001**, *1*, 323−328.

(12) (a) Tang, B. Z. *Polym. Prepr.* **2002**, *43* (1), 48−49. (b) Li, B. S.; Cheuk, K. K. L.; Zhou, J.; Xie, Y.; Tang, B. Z. *Polym. Mater. Sci. Eng.* **2001**, *85*, 401−402. (c) Li, B. S.; Cheuk, K. K. L.; Zhou, J.; Xie, Y.; Cha, J. A. K.; Xiao, X.; Tang, B. Z. *Polym. Prepr.* **2001**, *42* (1), 543−544.

(13) (a) Bianconi, P. A.; Weidman, T. W. *J. Am. Chem. Soc.* **1988**, *110*, 2342−2344. (b) Bianconi, P. A.; Schilling, F. C.; Weidman, T. W. *Macromolecules* **1989**, *22*, 1697−1704. (c) Smith, D. A.; Freed, C. A.; Bianconi, P. A. *Chem. Mater.* **1993**, *5*, 245−247.

(14) Various structures have been proposed for the polysilynes prepared under different conditions. In an early structural model, it was suggested that the polysilynes possessed a sheetlike structure consisting of annelated rings of different sizes, primarily six- and seven-membered silacyclics.[13] Dendritic structures were later proposed for a group of homo- and copolymers containing silicon atoms connected to three and four other silicon atoms: (a) Maxka, J.; Chrusciel, J.; Sasaki, M.; Matyjaszewski, K. *Macromol. Symp.* **1994**, *77*, 79−92. A quasi-linear random model was put forward for the structure of *n*-hexyl substituted polysilenes containing *n*-hexylsilyne branching points: (b) VanWalree, C. A.; Cleij, T. J.; Jenneskens, L. W.; Vlietstra, E. J.; vanderLaan, G. P.; deHaas, M. P.; Lutz, E. T. G. *Macromolecules* **1996**, *29*, 7362−7373. A study on water-soluble polysilynes revealed their novel thermoresponsive behavior, and on the basis of the experimental observations as well as the semiempirical theoretical calculations, a random backbone structure was postulated: (c) Cleij, T. J.; Tsang, S. K. Y.; Jenneskens, L. W. *Macromolecules* **1999**, *32*, 3286−3294. This random backbone structure model was further supported by a recent Monte Carlo simulation study, which showed that the random structure of the polysilyne networks contained cyclic substructures, linear chains, and branching points: (d) Vink, R. L. C.; Barkema, G. T.; vanWalree, C. A.; Jenneskens, L. W. *J. Chem. Phys.* **2002**, *116*, 854−859.

(15) (a) Watanabe, A.; Komatsubara, T.; Matsuda, M.; Yoshida, Y.; Tagawa, S. *Macromol. Chem. Phys.* **1995**, *196*, 1229−1240. (b) Watanabe, A.; Tsutsumi, Y.; Matsuda, M. *Synth. Met.* **1995**, *74*, 191−196. (d) Watanabe, A.; Sato, T.; Matsuda, M. *Jpn. J. Appl. Phys.* **2001**, *40*, 6457−6463.

(16) (a) Hecht, S.; Frechet. J. M. J. *Angew. Chem., Int. Ed.* **2001**, *40*, 74−91. (b) Voit, B. *J. Polym. Sci. Polym. Chem.* **2000**, *38*, 2505−2525. (c) Hawker, C. J. *Adv. Polym. Sci.* **1999**, *147*, 113−160. (d) Hult, A.; Johansson, M.; Malmstrom, E. *Adv. Polym. Sci.* **1999**, *143*, 1−34. (e) Burchard, W. *Adv. Polym. Sci.* **1999**, *143*, 113−194. (f) Matthews, O. A.; Shipway, A. N.; Stoddart, J. F. *Prog. Polym. Sci.* **1998**, *23*, 1−56. (g) Tomalia, D. A.; Durst, H. D. *Top. Curr. Chem.* **1993**, *165*, 193−313.

(17) (a) Crooks, R. M. *Chem. Phys. Chem.* **2001**, *2*, 644−654. (b) Frey, H.; Schlenk, C. *Top. Curr. Chem.* **2000**, *210*, 69−129. (c) Bischoff, R.; Cray, S. E. *Prog. Polym. Sci.* **1998**, *24*, 185−219. (d) Cuadrado, I.; Moran, M.; Casado, C. M.; Alonso, B.; Losada, J. *Coord. Chem. Rev.* **1999**, *195*, 395−445. (e) Frey, H.; Lach, C.; Lorenz, K. *Adv. Mater.* **1998**, *10*, 279−293. (f) Ardoin, N.; Astruc, D. *Bull. Soc. Chim. Fr.* **1995**, *132*, 875−909. (g) West, R.; Oka, K.; Takahashi, H.; Miller, M.; Gunji, T. *ACS Symp. Ser.* **1994**, *572*, 92−101. (h) Sakurai, H.; Sakamoto, K.; Funada, Y.; Yoshida, M. *ACS Symp. Ser.* **1994**, *572*, 8−17.

(18) (a) Whitmarsh, C. W.; Interrante, L. V. *Organometallics* **1991**, *10*, 1336−1344. (b) Rushkin, I. L.; Shen, Q.; Lehman, S. E.; Interrante, L. V. *Macromolecules* **1997**, *30*, 3141−3146. (c) Sorarù, G. D.; Liu, Q.; Interrante, L. V.; Apple, T. *Chem. Mater.* **1998**, *10*, 4047−4054.

(19) (a) Ohshita, J. *J. Synth. Org. Chem. Jpn.* **2001**, *59*, 11−22. (b) Yamaguchi, Y. *Synth. Met.* **1996**, *82*, 149−153. (c) Yamaguchi, S.; Tamao, K. *Bull. Chem. Soc. Jpn.* **1996**, *69*, 2327−2334. (d) Miller, R. D.; Sooriyakumaran, R. *J. Polym. Sci. Part C: Polym. Lett.* **1987**, *25*, 321−325.

(20) (a) *Macromolecular Systems: Microscopic Interactions and Macroscopic Properties*; Hoffmann, H., Schwoerer, M., Vogtmann, T., Eds.; Wiley-VCH: Weinheim, 2000.

(21) (a) Seyferth, D. In *Silicon-Based Polymer Science: a Comprehensive Resource*; Zeigler, J. M., Fearon, F. W. G., Eds.; American Chemical Society: Washington, DC, 1990; Chapter 31, pp 565−592. (b) *Advanced Structural and Functional Materials*; Bunk, W. G. J., Ed.; Springer-Verlag: Hong Kong, 1991. (c) *Metal-Containing Polymeric Materials*; Pittman, C. U., Jr., Ed.; Plenum Press: New York, 1996.

(22) (a) Tang, B. Z.; Petersen, R.; Foucher, D. A.; Lough, A.; Coombs, N.; Sodhi, R.; Manners, I. *J. Chem. Soc., Chem. Commun.* **1993**, 523−525. (b) Petersen, R.; Foucher, D. A.; Tang, B. Z.; Lough, A.; Raju, N. P.; Greedan, J. E.; Manners, I. *Chem. Mater.* **1995**, *7*, 2045−2053.

(23) "Polysilene" is a structure-based name according to the systematic nomenclature rules of IUPAC [e.g.: (a) Kabeta, K.; Shuto, K.; Sugi, S.-I.; Imai, T. *Polymer* **1996**, *37*, 4327−4331]. Its source-based name is "polysilane". Similarly, "poly(ferrocenylenesilene)" is a structure-based name [e.g.: (b) Matyjaszewski, K.; Miller, P. J.; Fossum, E.; Nakagawa, Y. *Appl. Organomet. Chem.* **1998**, *12*, 667−673. (c) Pannell, K. H.; Sharma, H. K. *Organometallics* **1997**, *16*, 3077−3079. (d) Nelson, J. M.; Nguyen, P.; Petersen, R.; Rengel, H.; Macdonald, P. M.; Lough, A. J.; Manners, I.; Raju, N. P.; Greedan, J. E.; Barlow, S.; O'Hare, D. *Chem. Eur. J.* **1997**, *3*, 573−584]. Its source-based name is "poly(ferrocenylsilane)". Although the source-based names are widely used, we chose to use the structure-based nomenclatures in order to keep consistency in naming the polymers and to make structural comparisons in this paper.

(24) (a) Foucher, D. A.; Tang, B. Z.; Manners, I. *J. Am. Chem. Soc.* **1992**, *114*, 6246−6248. (b) Foucher, D. A.; Honeyman, C. H.; Nelson, J. M.; Tang, B. Z.; Manners, I. *Angew. Chem., Int. Ed.* **1993**, *32*, 1709−1711. (c) Foucher, D. A.; Ziembinski, R.; Tang, B. Z.; Macdonald, P. M.; Massey, J.; Jaeger, C. R.; Vancso, G. J.; Manners, I. *Macromolecules* **1993**, *26*, 2878−2884. (d) Finckh, W.; Tang, B. Z.; Foucher, D. A.; Zamble, D. B.; Ziembinski, R.; Lough, A.; Manners, I. *Organometallics* **1993**, *12*, 823−829. (e) Rasburn, J.; Seker, F.; Kulbaba, K.; Klein, P. G.; Manners, I.; Vancso, G. J.; Macdonald, P. M. *Macromolecules* **2001**, *34*, 2884−2891. (f) Lammertink, R. G. H.; Hempenius, M. A.; Vancso, G. J.; Shin, K.; Rafailovich, M. H.; Sokolov, J. *Macromolecules* **2001**, *34*, 942−950. (g) Hempenius, M. A.; Vancso, G. J. *Macromolecules* **2002**, *35*, 2445−2447.

(25) For selected examples of reviews, see: (a) Nguyen, P.; Gomez-Elipe, P.; Manners, I. *Chem. Rev.* **1999**, *99*, 1515−1548. (b) Manners, I. *Angew. Chem., Int. Ed.* **1996**, *35*, 1603−1621. (c) Manners, I. *Adv. Organomet. Chem.* **1995**, *37*, 131−168.

(26) (a) Sun, Q.; Lam, J. W. Y.; Xu, K.; Xu, H.; Cha, J. A. P.; Wong, P. C. L.; Wen, G.; Zhang, X.; Jing, X.; Wang, F.; Tang, B. Z. *Chem. Mater.* **2000**, *12*, 2617−2624. (b) Sun, Q.; Xu, K.; Lam, J. W. Y.; Cha, J. A. P.; Zhang, X.; Tang, B. Z. *Mater. Sci. Eng. C* **2001**, *16*, 107−112. (c) Tang, B. Z.; Sun, Q.; Xu, K.; Peng, H.; Lam, J. W. Y.; Cha, J. A. K.; Luo, J.; Zhang, X. US Patent Appl. No. 10/106,752, 2002.

(27) (a) Sun, Q.; Tang, B. Z. *Polym. Prepr.* **1999**, *40* (2), 657−658. (b) Sun, Q.; Tang, B. Z. *Polym. Mater. Sci. Eng.* **2000**, *82*, 105−106. (c) Sun, Q.; Wen, G.; Zhang, X.; Tang, B. Z. *Polym. Mater. Sci. Eng.* **2000**, *82*, 107−108. (d) Sun, Q.; Tang, B. Z. *Polym. Mater. Sci. Eng.* **2000**, *82*, 109−110. (e) Sun, Q.; Xu, K.; Peng, H.; Tang, B. Z. *Polym. Mater. Sci. Eng.* **2002**, *86*, 89−90.

(28) (a) Xu, K.; Peng, H.; Sun, Q.; Dong, Y.; Salhi, F.; Luo, J.; Chen, J.; Huang, Y.; Zhang, D.; Xu, Z.; Tang, B. Z. *Macromolecules* **2002**, *35*, 5821−5834. (b) Peng, H.; Cheng, L.; Luo, J.; Xu, K.; Sun, Q.; Dong, Y.; Salhi, F.; Lee, P. P. S.; Chen, J.; Tang, B. Z. *Macromolecules* **2002**, *35*, 5349−5351. (c) Xu, K.; Tang, B. Z. *Chin. J. Polym. Sci.* **1999**, *17*, 397−402. (d) Tang, B. Z. *Polym. Prepr.* **2002**, *43* (1), 48−49.

(29) (a) Peng, H.; Luo, J.; Cheng, L.; Lam, J. W. Y.; Xu, K.; Dong, Y.; Zhang, D.; Huang, Y.; Xu, Z.; Tang, B. Z. *Opt. Mater.* **2002**, *21*, 315−320. (b) Lam, J. W. Y.; Luo, J.; Peng, H.; Xie, Z.; Xu, K.; Dong, Y.; Cheng, L.; Qiu, C.; Kwok, H. S.; Tang, B. Z. *Chin. J. Polym. Sci.* **2001**, *19*, 585−590. (c) Tang, B. Z.; Xu, K.; Peng, H.; Sun, Q.; Luo, J. US Patent Appl. No. 10/109,316, 2002.

(30) Reddinger, J. L.; Reynolds, J. R. *Adv. Polym. Sci.* **1999**, *145*, 57−122. (b) Segura, J. L. *Acta Polym.* **1998**, *49*, 319−344. (c)

Goodson, F. E.; Wallow, T. I.; Novak, B. M. *Macromolecules* **1998**, *31*, 2047−2056. (d) Tarkka, R. M.; Chen, X. L.; Jenekhe, S. A. *ACS Symp. Ser.* **1997**, *672*, 475−494. (e) Higgins, S. J. *Chem. Soc. Rev.* **1997**, *26*, 247−257. (f) Nishide, H. *ACS Symp. Ser.* **1996**, *644*, 247−257. (g) Schluter, A. D.; Wegner, G. *Acta Polym.* **1993**, *44*, 59−69. (h) Roncali, J. *Chem. Rev.* **1992**, *92*, 711−738.

(31) Cowie, J. M. G. *Polymers: Chemistry & Physics of Modern Materials*, 2nd ed.; Blackie Academic and Professional: London, 1991; Chapter 16, pp 362−398.

(32) (a) Kong, X.; Lam, J. W. Y.; Tang, B. Z. *Macromolecules* **1999**, *32*, 1722−1730. (b) Kong, X.; Tang, B. Z. *Chem. Mater.* **1998**, *10*, 3352−3363. (c) Tang, B. Z.; Kong, X.; Wan, X.; Peng, H.; Lam, W. Y.; Feng, X.; Kwok, H. S. *Macromolecules* **1998**, *31*, 2419−2432. (d) Tang, B. Z.; Kong, X.; Feng, X.-D. *Chin. J. Polym. Sci.* **1999**, *17*, 289−294. (e) Kong, X.; Wan, X.; Kwok, H. S.; Feng, X.-D.; Tang, B. Z. *Chin. J. Polym. Sci.* **1998**, *16*, 185−192.

(33) (a) Grayson, S. M.; Frechet, J. M. J. *Macromolecules* **2001**, *34*, 6542. (b) Muchtar, Z.; Schappacher, M.; Deffieux, A. *Macromolecules* **2001**, *34*, 7595. (c) Uhrich, K. E.; Hawker, C. J.; Frechet, J. M. J.; Turner, S. R. *Macromolecules* **1992**, *25*, 4583.

(34) Silverstern, R. M.; Webster, F. X. *Spectrometric Identification of Organic Compounds*, 6th ed.; Wiley: 1998; Chapter 3, pp 71−143.

(35) Konstantinovic, C.; Simova, S.; Rufinska, A.; Ratkovic, Z.; Predojevic, J.; Rufinska, A.; Gojkovic, S. *Ind. J. Chem. B* **1996**, *35*, 960−964.

(36) (a) Aihara, S.; Kamata, N.; Umeda, M.; Kanezaki, S. I.; Nagumo, K.; Terunuma, D.; Yamada, K. *Opt. Rev.* **1999**, *6*, 393−395. (b) Matsumoto, N. *Jpn. J. Appl. Phys.* **1998**, *37*, 5425−5436. (c) Steinmetz, M. G. *Chem. Rev.* **1995**, *95*, 1527−1588.

(37) (a) Chen, H.; Lam, J. W. Y.; Luo, J.; Ho, Y.; Tang, B. Z.; Zhu, D.; Wong, M.; Kwok, H. S. *Appl. Phys. Lett.* **2002**, *81*, 574−576. (b) Luo, J.; Xie, Z.; Lam, J. W. Y.; Cheng, L.; Chen, H.; Qiu, C.; Kwok, H. S.; Zhan, X.; Liu, Y.; Zhu, D.; Tang, B. Z. *Chem. Commun.* **2001**, 1740−1741. (c) Tang, B. Z.; Zhan, X.; Yu, G.; Lee, P. P. S.; Liu, Y.; Zhu, D. *J. Mater. Chem.* **2001**, *11*, 2874−2978.

(38) (a) Lam, J. W. Y.; Dong, Y.; Luo, J.; Cheuk, K. K. L.; Xie, Z.; Tang, B. Z. *Thin Solid Films* **2002**, *417*, 143−146. (b) Huang, Y.; Law, C.; Ge, W.; Lam, J. W. Y.; Tang, B. Z. *J. Lumin.* **2002**, *99*, 161−168. (c) Lam, J. W. Y.; Luo, J.; Peng, H.; Xie, Z.; Xu, K.; Dong, Y.; Cheng, L.; Qiu, C.; Kwok, H. S.; Tang, B. Z. *Chin. J. Polym. Sci.* **2001**, *19*, 585−590. (d) Huang, Y.; Ge, W.; Lam, J. W. Y.; Cheuk, K. K. L.; Tang, B. Z. *Mater. Sci. Eng. B* **2001**, *85*, 242−246. (e) Huang, Y.; Ge, W.; Lam, J. W. Y.; Cheuk, K. K. L.; Tang, B. Z. *Mater. Sci. Eng. B* **2001**, *85*, 122−125. (f) Huang, Y.; Ge, W.; Lam, J. W. Y.; Cheuk, K. K. L.; Tang, B. Z. *Mater. Sci. Eng. B* **2001**, *85*, 118−121. (g) Lee, P. P. S.; Geng, Y.; Kwok, H. S.; Tang, B. Z. *Thin Solid Films* **2000**, *363*, 149−151. (h) Huang, Y.; Lam, J. W. Y.; Cheuk, K. K. L.; Ge, W.; Tang, B. Z. *Thin Solid Films* **2000**, *363*, 146−148. (i) Xu, H.; Sun, Q.; Lee, P. P. S.; Kwok, H. S.; Tang, B. Z. *Thin Solid Films* **2000**, *363*, 143−145.

(39) (a) Friend, R. H.; Gymer, R. W.; Holmes, A. B.; Burroughes, J. H.; Marks, R. N.; Taliani, C.; Bradley, D. D. C.; Dos Santos, D. A.; Bredas, J. L.; Logdlund, M.; Salaneck, W. R. *Nature* **1999**, *397*, 121−128. (b) Li, X.-C.; Moratti, S. C. In *Photonic Polymer Systems*; Wise, D. L., Wnek, G. E., Trantolo, D. J., Cooper, T. M., Gresser, J. D., Eds.; Marcel Dekker: Hong Kong, 1998; Chapter 10, pp 335−371.

(40) (a) Pugh, C.; Kiste, A. L. *Prog. Polym. Sci.* **1997**, *22*, 601−691. (b) Shiota, A.; Ober, C. K. *Prog. Polym. Sci.* **1997**, *22*, 975−1000. (c) Percec, V.; Tomazos, D. *Adv. Mater.* **1992**, *4*, 548−561. (d) Daly, W. H.; Negulescu, I. I.; Russo, P. S.; Poche, D. S. *ACS Symp. Ser.* **1992**, *493*, 292−299.

(41) Rasburn, J.; Petersen, R.; Jahr, T.; Rulkens, R.; Manners, I.; Vancso, G. J. *Chem. Mater.* **1995**, *7*, 871−877.

(42) (a) Tang, B. Z.; Geng, Y.; Lam, J. W. Y.; Li, B.; Jing, X.; Wang, X.; Wang, F.; Pakhomov, A. B.; Zhang, X. X. *Chem. Mater.* **1999**, *11*, 1581−1589. (b) Tang, B. Z.; Geng, Y.; Sun, Q.; Zhang, X.; Jing, X. *Pure Appl. Chem.* **2000**, *72*, 157−162.

(43) (a) Ginzburg, M.; MacLachlan, M. J.; Yang, S. M.; Coombs, N.; Coyle, T. W.; Raju, N. P.; Greedan, J. E.; Herber, R. H.; Ozin, G. A.; Manners, I. *J. Am. Chem. Soc.* **2002**, *124*, 2625−2639. (b) Massey, J. A.; Winnik, M. A.; Manners, I.; Chan, V. Z. H.; Ostermann, J. M.; Enchelmaier, R.; Spatz, J. P.; Moller, M. *J. Am. Chem. Soc.* **2001**, *123*, 3147−3148. (c) MacLachlan, M. J.; Ginzburg, M.; Coombs, N.; Raju, N. P.; Greedan, J. E.; Ozin, G. A.; Manners, I. *J. Am. Chem. Soc.* **2000**, *122*, 3878−3891. (d) MacLachlan, M. J.; Ginzburg, M.; Coombs, N.; Coyle, T. W.; Raju, N. P.; Greedan, J. E.; Ozin, G. A.; Manners, I. *Science* **2000**, 287, 1460−1463.

(44) (a) Crooks, R. M.; Zhao, M. Q.; Sun, L.; Chechik, V.; Yeung, L. K. *Acc. Chem. Res.* **2001**, *34*, 181−190. (b) Penner, R. M. *Acc. Chem. Res.* **2000**, *33*, 78−86. (c) Rao, C. N. R.; Kulkarni, G. U.; Thomas, P. J.; Edwards, P. P. *Chem. Soc. Rev.* **2000**, *29*, 27−35.

(45) (a) *Handbook of X-ray Photoelectron Spectroscopy: a Reference Book of Standard Spectra for Identification and Interpretation of XPS Data*; Chastain, J., Ed.; Physical Electronics Division, Perkin-Elmer Corp.: Eden Prairie, MN, 1992. (b) *Practical Surface Analysis*; Briggs, D., Seah, M. P., Eds.; Wiley: Chichester, U.K., 1990.

(46) Hellwege, K.-K.; Hellwege, A. M. *Landolt-Börnstern: Numerical Data and Functional Relationships in Science and Technology*; Springer-Verlag: New York, 1970; New Series, Group III, Vol. 4, Part a, Figure 59.

(47) (a) Yan, X. H.; Liu, G. J.; Liu, F. T.; Tang, B. Z.; Peng, H.; Pakhomov, A. B.; Wong, C. Y. *Angew. Chem., Int. Ed.* **2001**, *40*, 3593−3596. (b) Lopez, D.; Cendoya, I.; Mijangos, C.; Julia, A.; Ziolo, R. F.; Tejada, J. *Macromol. Symp.* **2001**, *166*, 173−178. (c) Liu, G. J.; Ding, J. F.; Hashimoto, T.; Kimishima, K.; Winnik, F. M.; Nigam, S. *Chem. Mater.* **1999**, *11*, 2233−2240. (d) Winnik, F. M.; Morneau, A.; Mika, A. M.; Childs, R. F.; Roig, A.; Molins, E.; Ziolo, R. F. *Can. J. Chem.* **1998**, *76*, 10−17. (e) Zhang, L.; Papaefthymiou, G. C.; Ying, J. Y. *J. Appl. Phys.* **1997**, *81*, 6892−6900. (f) Zhang, L.; Papaefthymiou, G. C.; Ziolo, R. F.; Ying, J. Y. *Nanostruct. Mater.* **1997**, *9*, 185−188.

(48) (a) Douy, A. *Int. J. Inorg. Mater.* **2001**, *3*, 699−707. (b) Simon, P. F. W.; Ulrich, R.; Spiess, H. W.; Wiesner, U. *Chem. Mater.* **2001**, *13*, 3464−3486. (c) Nedeljkovic, J. M. *Mater. Sci. Forum* **2000**, *352*, 79−85. (d) Kroke, E.; Li, Y. L.; Konetschny, C.; Lecomte, E.; Fasel, C.; Riedel, R. *Mater. Sci. Eng. R* **2000**, *26*, 97−199. (e) Breulmann, M.; Davis, S. A.; Mann, S.; Hentze, H. P.; Antonietti, M. *Adv. Mater.* **2000**, *12*, 502−506. (f) Vollath, D.; Szabo, D. V.; Fuchs, J. *Nanostruct. Mater.* **1999**, *12*, 433−438. (g) Suryanarayana, C. *Int. Mater. Rev.* **1995**, *40*, 41−64.

(49) (a) Safarik, I.; Safarikova, M. *Monatsh. Chem.* **2002**, *133*, 737−759. (b) Schneider, J. J.; Czap, N.; Hagen, J.; Engstler. J.; Ensling, J.; Gutlich, P.; Reinoehl, U.; Bertagnolli, H.; Luis, F.; de Jongh, L. J.; Wark, M.; Grubert, G.; Hornyak, G. L.; Zanoni, R. *Chem. Eur. J.* **2000**, *6*, 4305−4321. (c) Majetich, S. A.; Jin, Y. *Science* **1999**, *284*, 470−473. (d) Shi, J.; Gider, S.; Babcock, K.; Awschalom, D. D. *Science* **1996**, *271*, 937−941. (e) Taft, K. L.; Papaefthymiou, G. C.; Lippard, S. J. *Science* **1993**, *259*, 1302−1305.

(50) (a) *Power Electronics in Transportation*; Power Electronics Society: Piscataway, NJ, 1998. (b) Chen, C.-W. *Magnetism and Metallurgy of Soft Magnetic Materials*; Dover: New York, 1986.

(51) (a) Kemeny, T.; Kaptas, D.; Kiss, L. F.; Balogh, J.; Vincze, I.; Szabo, S.; Beke, D. L. *Hyperfine Interact.* **2000**, *130*, 181−219. (b) McHenry, M. E.; Willard, M. A.; Laughlin, D. E. *Prog. Mater. Sci.* **1999**, *44*, 291−433.

MA021529E